International Journal of Electrical and Computer Engineering (IJECE)
Vol. 3, No. 6, December 2013, pp. 831~848
ISSN: 2088-8708

Effect of Functionally Graded Material of Disc Spacer with Presence of Multi-Contaminating Particles on Electric Field inside Gas Insulated Bus Duct

M.A. Abd Allah[1], Sayed A. Ward[2], Amr A. Youssef[3]
Electrical Engineering Department, Faculty of Engineering at Shoubra
Benha University, Cairo, Egypt
e-mail: eng_power_amr2011@yahoo.com

Article Info

Article history:

Received Sep 10, 2013
Revised Oct 19, 2013
Accepted Nov 8, 2013

Keyword:

Disc Spacer
Electric Field
FEM
FGM
Multi-particles
Triple junction

ABSTRACT

Solid insulators play a crucial role of electrical insulation in gas insulated power equipment. In order to improve the insulation performance of the solid insulators, two technical points should be considered, the first is the improvement of the insulation performance and the second is the control of the electric field distribution in and around the solid insulating spacers. These techniques lead to a more complicated structure of the equipment and increase the manufacturing cost. Thus, it is necessary to propose a new concept on solid spacers with keeping their simple structure and configuration. In this paper, a functionally graded material (FGM) is proposed to minimize the electric field distribution around the spacer, specially, on triple junction point, which was one of the important factors dominating a long-term insulating property of solid delectric. Finite Element Method (FEM) has been used throughout this work, for its favorable accuracy, to calculate the electric field distribution inside the bus duct. The effect of hemi-spherical radius and length of particle on maximum electric field at triple junction point is also discussed. Electric field relaxation effect (EFGM / Euniform) by introduction of the U-shape FGM spacer is also presented. The electric field distribution along the surface of FGM of disc spacer with presence of multi-contaminating particles at various positions is presented.

Corresponding Author:

Amr A. Youssef,
Electrical Engineering Department, Faculty of Engineering at Shoubra,
Benha University, Cairo, Egypt
e-mail: eng_power_amr2011@yahoo.com

1. INTRODUCTION

The computation of electric field is complex and it is usually difficult to find an exact solution. Several numerical techniques have been increasingly employed to solve such practical problems since the availability of high performance computers [1, 2]. The advantage of the application of numerical methods has many advantages compared to analytical methods such as computable accuracy, simplicity and low cost.

The finite element method (FEM) is used in this paper for its favorable accuracy, when applied to high voltage problems.

2. ELECTRIC FIELD CALCULATIONS

FEM one of the efficient technique for solving field problems is used to determine the electric field distribution on the spacer's surface. FEM concerns itself with minimization of the energy within the whole

field region of interest, whether the field is electric or magnetic, of Laplacian or Poisson type, by dividing the region into triangular elements for two dimensional problems or tetrahedrons for three dimensional problems. Under steady state the electrostatic field within anisotropic dielectric material, assuming a Cartesian coordinate system, and Laplacian field, the electrical energy W stored within the whole volume U of the region considered is [3]:

$$W = \frac{1}{2}\int_U \varepsilon \left| grad\ (V) \right|^2 dU \tag{1}$$

$$W = \frac{1}{2}\iiint_U \left[\varepsilon_x \left(\frac{\partial V_x}{\partial x} \right)^2 + \varepsilon_y \left(\frac{\partial V_y}{\partial y} \right)^2 + \varepsilon_z \left(\frac{\partial V_z}{\partial z} \right)^2 \right] dxdydz \tag{2}$$

Furthermore, for GIS arrangement, when we consider the field behaviour at minute level the problem can be treated as two dimensional (2D). The total stored energy within this area-limited system is now given according to [3]:

$$\frac{W}{\varphi} = \frac{1}{2} * \varepsilon \iint \left[\left(\frac{\partial V_x}{\partial x} \right)^2 + \left(\frac{\partial V_y}{\partial y} \right)^2 \right] dxdy \tag{3}$$

Where (W/φ) is thus an energy density perelementary area dA. Before applying any minimization criteria based upon the above equation, appropriate assumptions about the potential distribution V(x, y, z) must be made. It should be emphasized that this function is continuous and a finite number of derivatives may exist. As it will be impossible to find a continuous function for the whole area A, an adequate discretization must be made. So all the area under consideration is subdivided into triangular elements hence [3]:

$$\frac{W}{\varphi} = \frac{1}{2} * \varepsilon * \sum_{i=1}^{n} \left[\left(\frac{\partial V_x}{\partial x} \right)^2 + \left(\frac{\partial V_y}{\partial y} \right)^2 \right] * A_i \tag{4}$$

Where n is the total number of elements and Ai is the area of the ith triangle element. So the formulation regarding the minimization of the energy within the complete system may be written as [3]:

$$\frac{\partial X}{\partial \{V(x, y)\}} = 0; \quad Where \quad X = \frac{w}{\varphi} \tag{5}$$

The result is an approximation for the electrostatic potential for the nodes at which the unknown potentials are to be computed. Within each element the electric field strength is considered to be constant and the electric field strength is calculated as [3]:

$$\vec{E} = -\vec{I}\ \frac{\partial V(x, y)}{\partial x} - \vec{J}\ \frac{\partial V(x, y)}{\partial y} \tag{6}$$

The electric field is calculated with using the Finite Element Method (FEM) throughout this work. The Finite Element Method Magnetics (FEMM) Package is used to simulate the problems and to calculate the electric field inside gas insulated switchgear and gas insulated bus ducts as disscussed in this paper. FEMM is a finite element package for solving 2D planar and axi-symmetric problems in electrostatics and in low frequency magnetic [4].

3. MODELING OF GAS INSULATED BUS DUCT

Gas insulated bus duct consists of an aluminum conductor supported by a disc-spacer with an aluminum enclosure, as shown in Figure 1. All dimensions of gas insulated bus duct with coating and disc-spacer are given in millimeter as shown in the figure. Disc-spacer is made of epoxy material with width 30mm and relative permativity (εr=4.5). Diameters of the enclosure and conductor are 152mm, 55mm respectively. The void is been filled with SF6 gas. The analysis is done by using two concentric cylinder of

infinite length as shown in Figure 1. The voltage on the inner conductor of GIBD considered is taken as 1V. For any applied voltage the values of the electric fields can be proportioned.

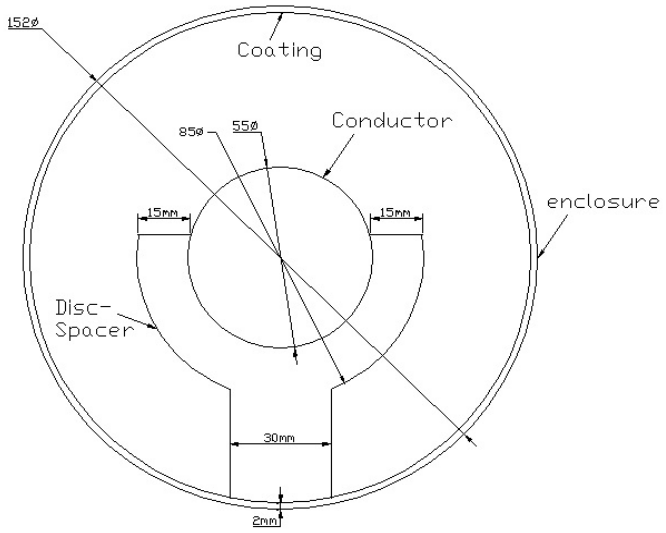

Figure 1. Gas insulated bus duct with disc-spacer of epoxy material

3.1. Electric Field Distribution Around Earthed Particle Contamination which Adhered to Disc-Spacer

Figure 2 shows gas insulated bus duct with earthed particle contamination which adhered to disc spacer. The particle length (L) is taken as 5mm and hemi-spherical radius (r) as 0.5mm. The distance between spacer and particle contamination (dps) is taken as zero mm.

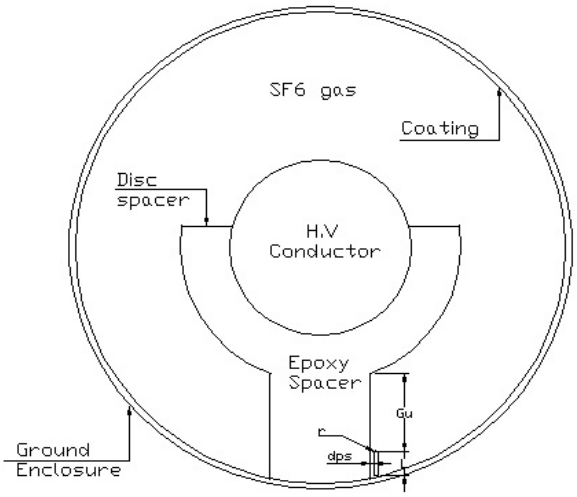

Figure 2. Gas insulated bus duct with earthed particle contamination which adhered to disc spacer

The electric potential distribution along gap with disc spacer and earthed particle adhered to it inside gas insulated bus duct is shown in Figure 3. It is observed that the voltage increases gradually from 0 volt at ground enclosure until it reaches 1V at high voltage conductor.

The electric field distribution around earthed contaminating particle which adhered to disc spacer inside GIBD is shown in Figure 4. It is clear that the electric field value is a maximum at triple junction, point (c), then the field value decreases gradually far from the particle until it reaches a certain value then it

begins to increase slightly nearest to the high voltage conductor. Figure 5 shows the electric field intensity lines.

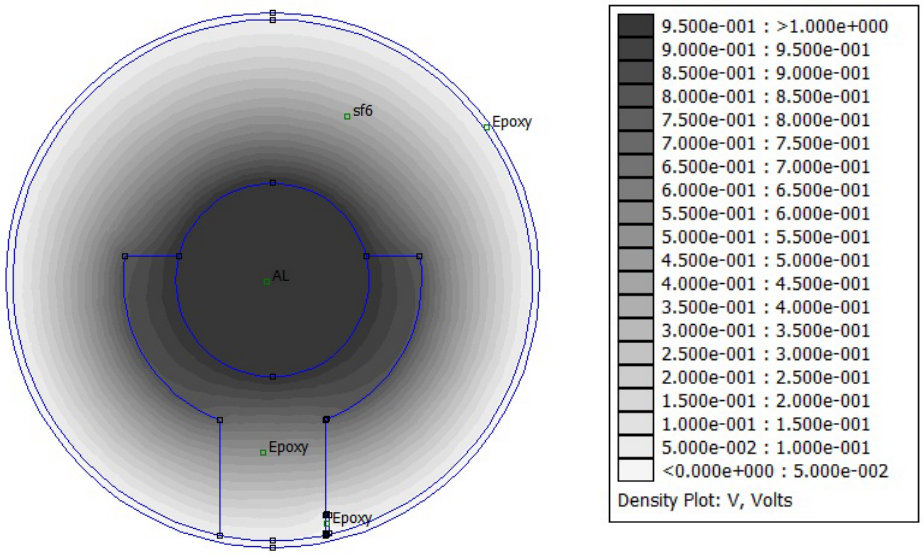

Figure 3. Electric Potential distribution along gap with disc spacer and earthed particle adhered to it inside gas insulated bus duct

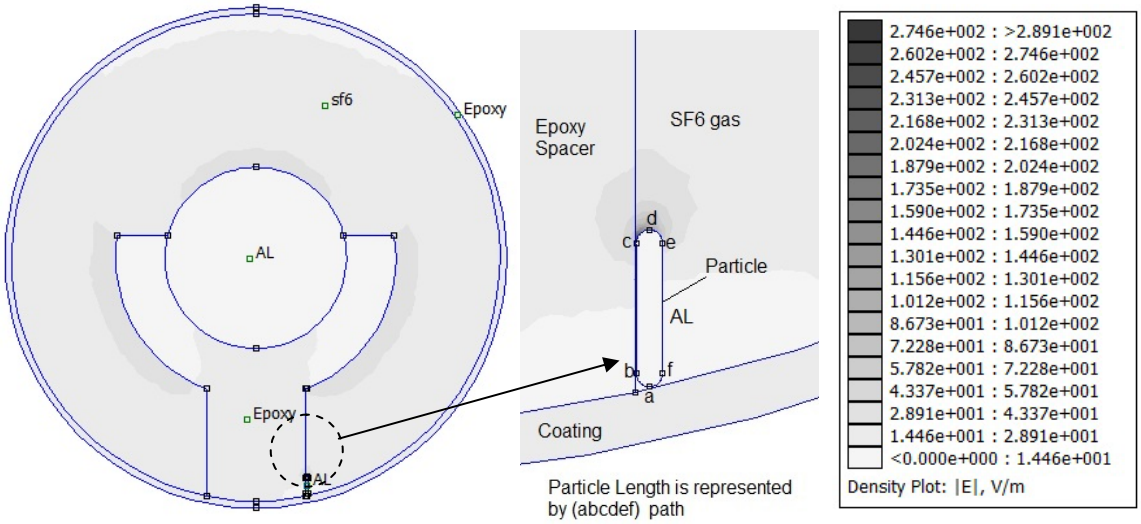

Figure 4. Electric field distribution around earthed contaminating particle which adhered to disc spacer inside gas insulated bus duct

The normal and tangential components of electric field along particle length which adhered to disc spacer inside gas insulated bus duct is shown in Figure 6. It can be observed that the tangential component of electric field is equal to zero along particle length. The normal component of electric field increases gradually from minimum value at lower tip of particle through negative side until it reaches maximum value at triple junction point(c) then it decreases along particle length from point c until it reaches the lower value at point (a). Finally, total component of electric field increases gradually from minimum value at point (a) of particle through point (b) until it reaches maximum value (289V/m) at triple junction point (c), after which

the field component decreases along particle length from point (d) to point (f) until it reaches the minimum value at point (a) of particle.

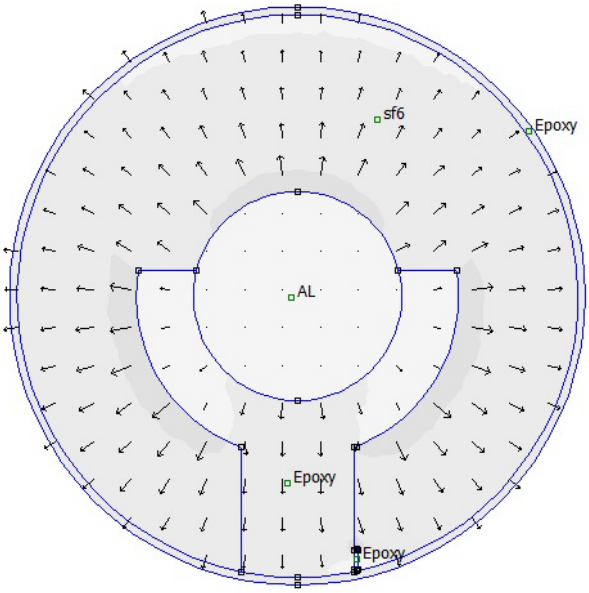

Figure 5. Electric field intensity lines inside gap of GIBD

Figure 7 shows magnitude, normal and tangential components of electric field distribution along upper gap space (Gu) from triple junction point (c) of particle up to high voltage conductor inside gas insulated bus duct. It is observed that the tangential component of electric field is about zero. The normal component of electric field decreases gradually through negative side from maximum value until it reaches a certain value through gap and then it slightly increased. The total component of electric field decreases gradually through positive side from maximum value at triple junction point (c) of particle until it reaches a certain value through gap and then it slightly increased near to the high voltage conductor.

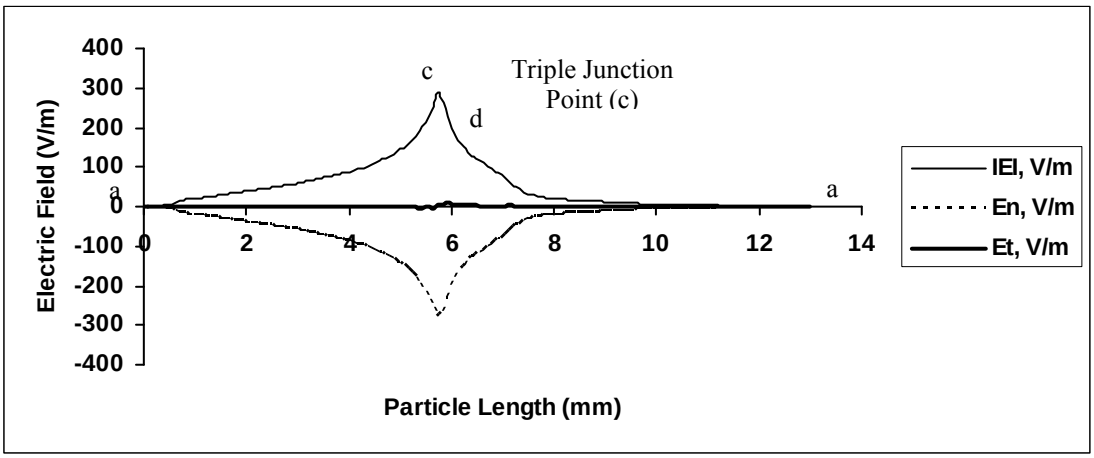

Figure 6. Electric field distribution along length of adhered particle to disc spacer inside gas insulated bus duct

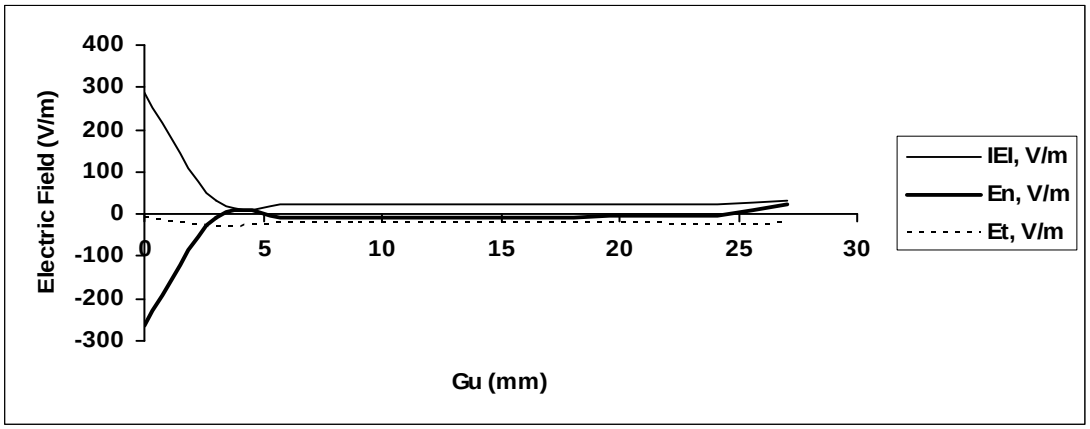

Figure 7. Electric field distribution along upper gap space (Gu) from triple junction point of particle up to high voltage conductor

(a) Effect of distance between particle and spacer on the electric field values

Figure 8 shows the electric field distribution along the particle length at different values of spacing between particle and spacer. it is noticed that the electric field along the particle length decreases as the distance between particle and spacer increases. The maximum electric field is observed at triple junction point of particle when it adhered to spacer. As the distance between particle and spacer increases, the maximum electric field is observed at hemi-spherical radius of particle from spacer side.

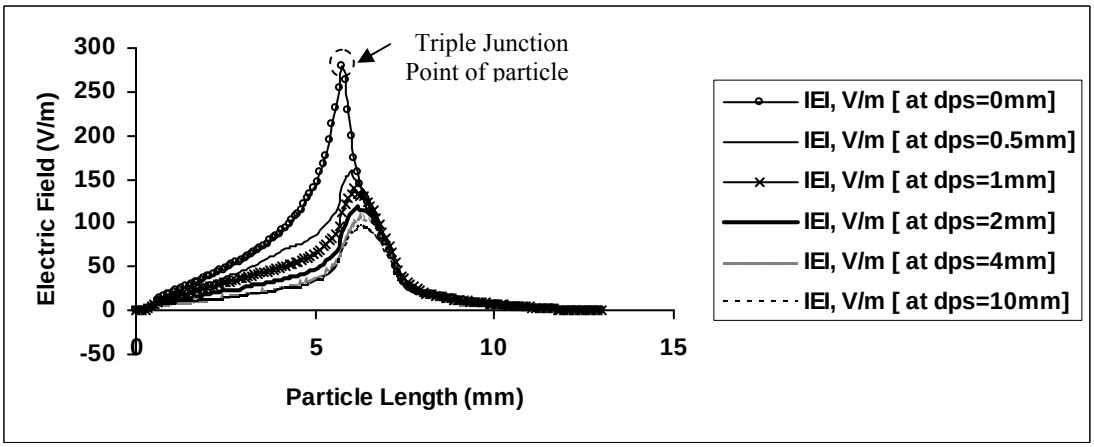

Figure 8. Electric field distribution along particle length at different values of spacing between particle and spacer

(b) Effect of hemi-spherical radius of particle on maximum electric field at triple junction point

The effect of hemi-spherical radius of particle on maximum electric field at triple junction point when the distance between particle and spacer (dps) is equal to zero and particle length (L=5mm) is shown in Figure 9. It is observed that the maximum electric field at triple junction point of particle decreases as hemi-spherical radius increases.

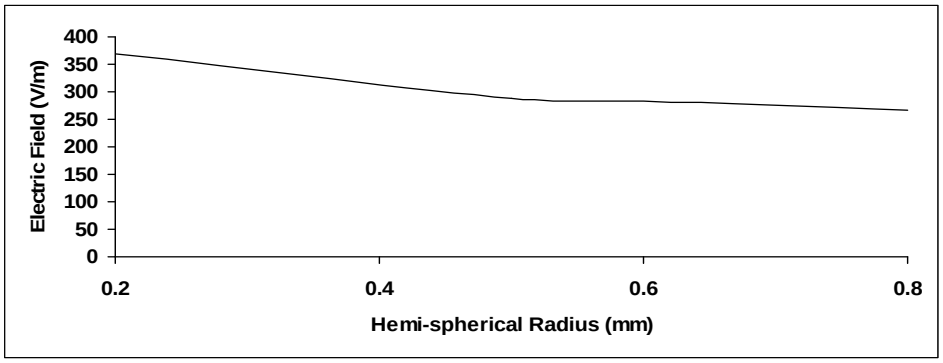

Figure 9. Maximum electric field at triple junction point of particle versus hemi-spherical radius at dps=zero and L=5mm

(c) Effect of particle length on maximum electric field at triple junction point

Figure 10 shows the effect of particle length on maximum electric field at triple junction point when distance between particle and spacer (dps) is equal to zero and particle radius (r=0.5mm). It is clear that the maximum electric field at triple junction point of particle increases as the particle length increases.

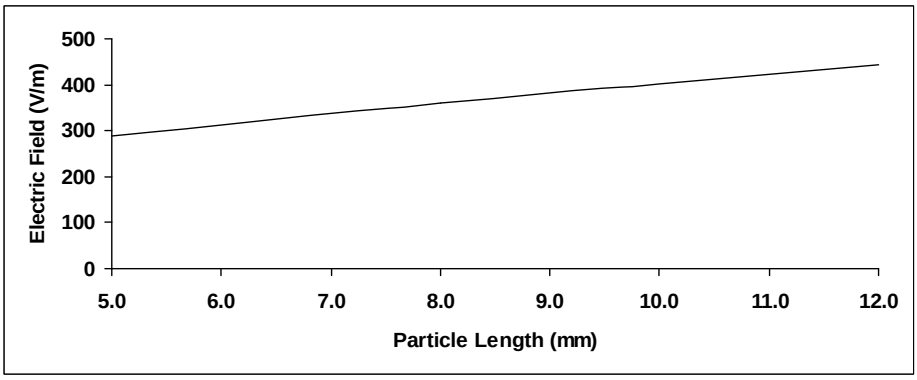

Figure 10. Maximum electric field at triple junction point versus particle length at dps=zero and r=0.5mm

3.2. Effect of Using Functionally Graded Material on Field Distribution

Recently, electric power equipment tends to be compact and be operated under higher voltage. The solid insulators play the crucial role in enhancing the insulation reliability and the compact design of gas insulated power equipment [5, 6]. In order to improve the insulation performance of the solid insulators two technical points can be considered. Firstly, a nano composite material can be used to improve the insulation performance [7,8]. Secondly, is the controlling of the electric field distribution in and around the solid insulating spacers [9, 10], which can be achieved by controlling the spacer shape, adding shield electrodes for electric field relaxation, introducting of an embedded electrode, and so on. These techniques for controlling the electric field lead to a more complicated structure of the equipment and increase the manufacturing cost. Thus, it is necessary to propose a new concept on solid spacers with keeping their simple structure and configuration.

A new concept for spacer insulation is used in this paper, called a functionally graded material (FGM). For relaxation of electric field stress, the FGM spacer should have spatial distribution of dielectric permittivity inside it. By the control of the distribution of dielectric permittivity, we could make the electric field distribution in and around the spacer more suitable. Thus, the fundamental investigations of the FGM spacer in electric power apparatus must be achieved [11-15]. The applicability of FGM for reducing the electric field stress on triple junction point with clean gap and also with particle contamination, which was one of the important factors dominating a long-term insulating property of the solid spacer, will be investigated.

3.2.1. Permittivity Distribution within Solid Spacer for Reducing Electric Stress

3.2.1.1. Shape Permittivity Distribution

In order to relax the electric field stress on electrode surface, the higher permittivity should be given around both anode and cathode surfaces compared with the other intermediate parts of solid insulator. It can be explained by the equivalent capacitor circuits of solid spacer configuration under static field as shown in Figure 11. The high permittivity capacitors in the vicinity of both sides of electrodes cause potential contingent to the inner low permittivity capacitor, decreasing the electric field in the vicinity of the electrode. Thus, U-shape distribution of the permittivity is suitable for the relaxation of electric field stress on electrode surface [16].

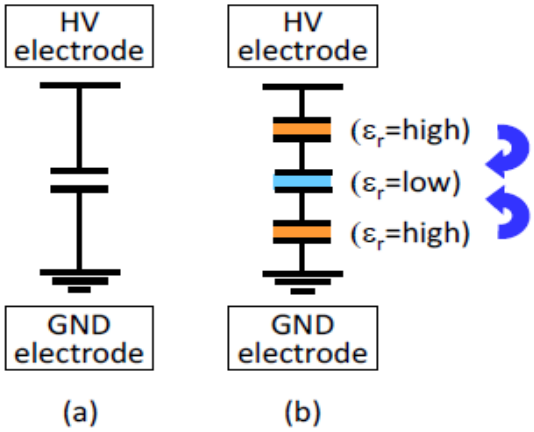

Figure 11. Equivalent capacitor circuits of solid spacer configuration,
(a) uniform permittivity, (b) permittivity distribution for reducing electric field in the vicinity of electrodes

3.2.1.2. Calculation Model for FGM Spacer

In order to confirm the field control effect of the proposed distribution of dielectric permittivity, we carried out the numerical calculation of electric field by finite element method (FEM).

Figure 12 shows the permittivity distribution (U-shape distribution) for the graded materials. This permittivity distribution was based on the optimized distribution of permittivity for minimizing the electric field stress on triple junction point with disc spacer calculation model by computer-aided optimization technique for the FGM solid insulators. Furthermore, in order to compare the performance, the spacer with uniform permittivity distribution (εr= 4.5) was also introduced.

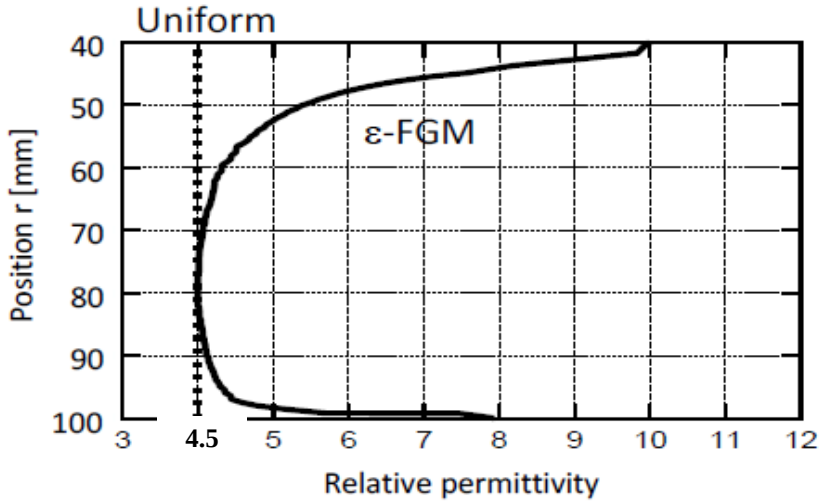

Figure 12. U-shape permittivity distribution of the spacer

(a) Electric field distribution along surface of FGM of disc spacer without particle contamination

Figure 13 shows the electric potential distribution along surface of FGM of disc- spacer inside gas insulated bus duct. It is observed that the voltage increases gradually from zero volt at ground enclosure through gap with disc spacer until it reaches 1 volt at high voltage conductor. The electric field distribution along surface of FGM of disc- spacer inside gas insulated bus duct is shown in Figure 14. It is clear that, the electric field increases gradually from lower triple junction point (E) until it reaches a certain value at point (D). From point (D) to point (C) along hemi-spherical radius of disc spacer, the electric field increases and then becomes approximately constant. From point (C) to point (B), the electric field decreases until it reaches minimum value at triple junction point (B) but it returns to increase until it reaches a certain value at point (A) along high voltage conductor.

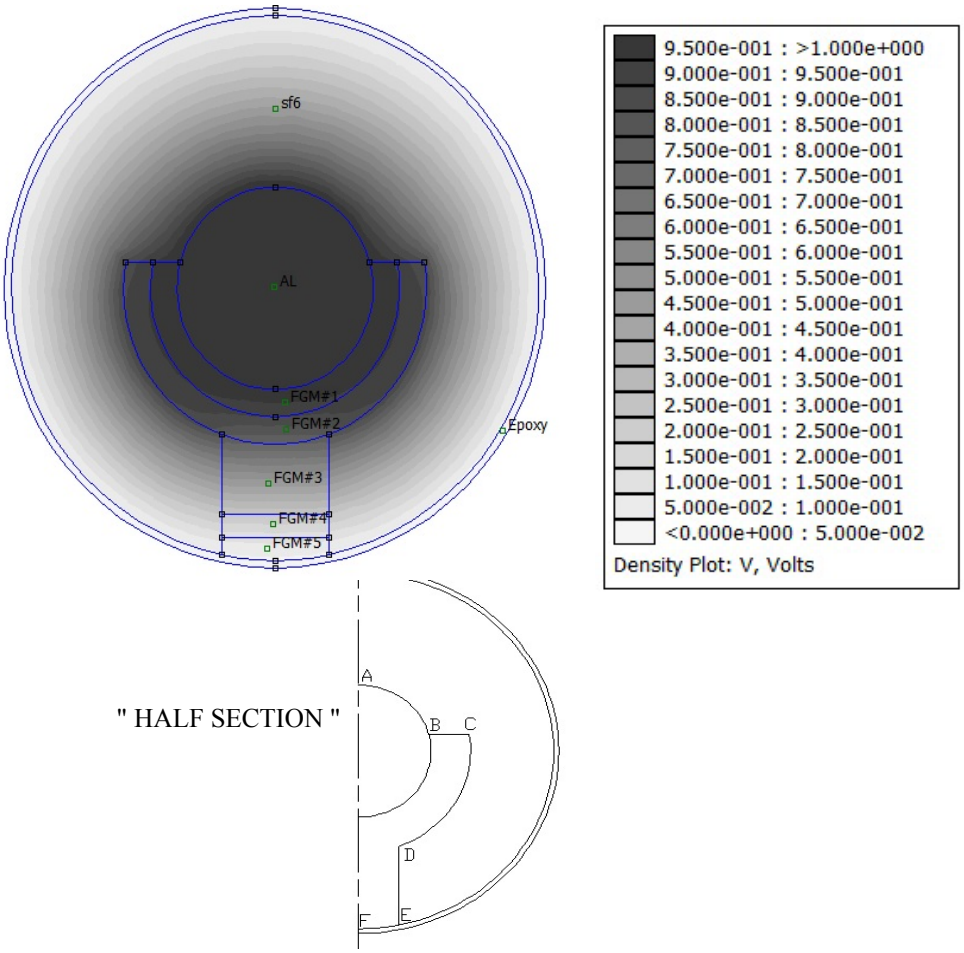

Figure 13. Electric Potential distribution along surface of FGM of disc spacer inside gas insulated bus duct

Figure 15 shows Electric field distribution along surface of uniform (Epoxy) and FGM of disc spacer inside gas insulated bus duct. It is seen that the electric field decreases gradually from point (A) until it reaches minimum value at point (B) of triple junction point at high voltage conductor. From point (B) to point (C), the electric field increases until it reaches a certain value. From point (C) to point (D), the electric field is approximately constant along hemi-spherical radius of high voltage conductor. From point (D) to point (E), the electric field decreases gradually until it reaches a certain value at triple junction point at ground enclosure. From point (E) to point (F), the electric field is slightly increased. It is found that the electric field strength on the both electrode surfaces in contact with solid insulators was reduced by introduction of the FGM spacers. In addition, the FGM spacer also allowed us to reduce the intensified field strength at distance 38 mm and 141 mm along (ABCDEF) path at triple junction points (B & E) at high voltage conductor and ground enclosure as shown in the figure.

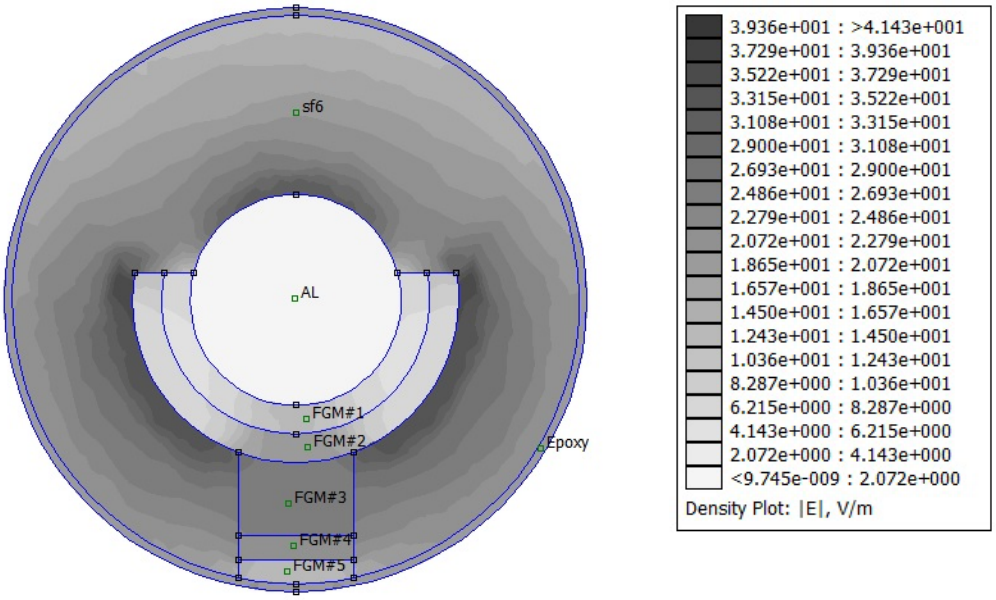

Figure 14. Electric field distribution along surface of FGM of disc spacer inside gas insulated bus duct

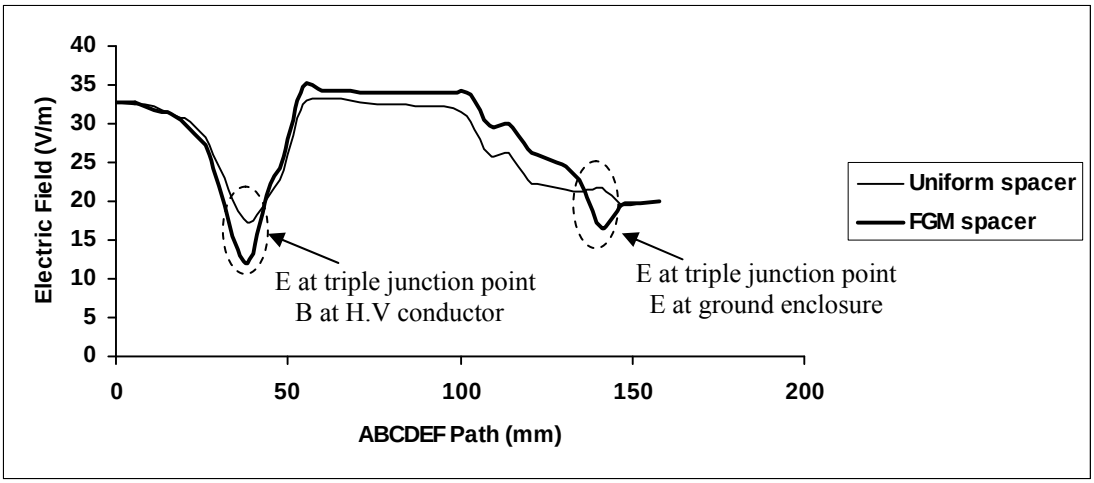

Figure 15. Electric field distribution along surface of uniform (Epoxy) and FGM of disc spacer inside gas insulated bus duct

Figure 16 shows the electric field relaxation effect on the electrode/spacer interface ($=E_{FGM}/E_{uniform}$). The result shows a relaxation effect of 0.69 on high voltage electrode/spacer interface and 0.75 on ground electrode/spacer interface by applying the U-shape FGM spacer.

(b) Electric field distribution along surface of FGM of disc spacer with single contaminating particle adhered to spacer

Figure 17 shows gas insulated bus duct with FGM of disc spacer and single contaminating particle adhered to spacer. Particle length (L) and radius (r) are taken as 5 mm and 0.5 mm respectively. Gu is defined as upper gap space from triple junction point of particle up to high voltage conductor.

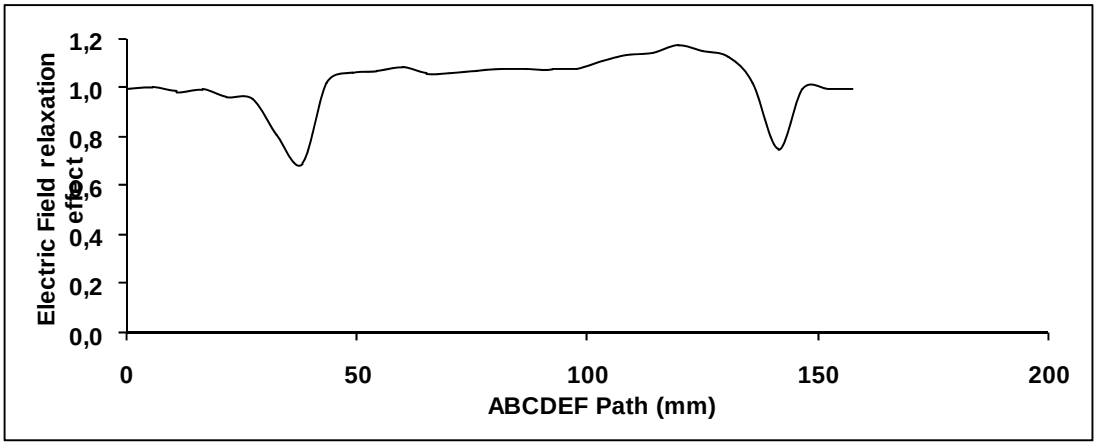

Figure 16. Electric field relaxation effect (E_{FGM} / $E_{uniform}$) by introduction of the U-shape FGM spacer

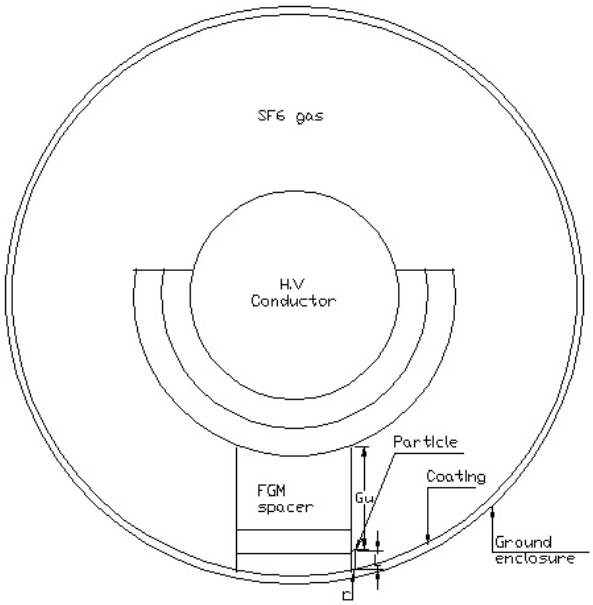

Figure 17. Gas insulated bus duct with FGM of disc spacer and single contaminating particle adhered to spacer

Figure 18 shows the electric potential distribution along surface of FGM of disc- spacer with single contaminating particle adhered to spacer inside gas insulated bus duct. It is found that the voltage increases gradually from zero volt at ground enclosure through gap with disc spacer until it reaches 1 volt at high voltage conductor.

Figure 19 shows the electric field distribution along surface of FGM of disc-spacer with single contaminating particle adhered to spacer inside gas insulated bus duct. From this figure, it is observed that, the electric field increases gradually from lower tip point (a) of particle until it reaches maximum value at triple junction point (c). From point (c) up to high voltage conductor, the electric field decreases gradually through gap as far from particle until it reaches a certain value and then it slightly increased as it approached from high voltage conductor.

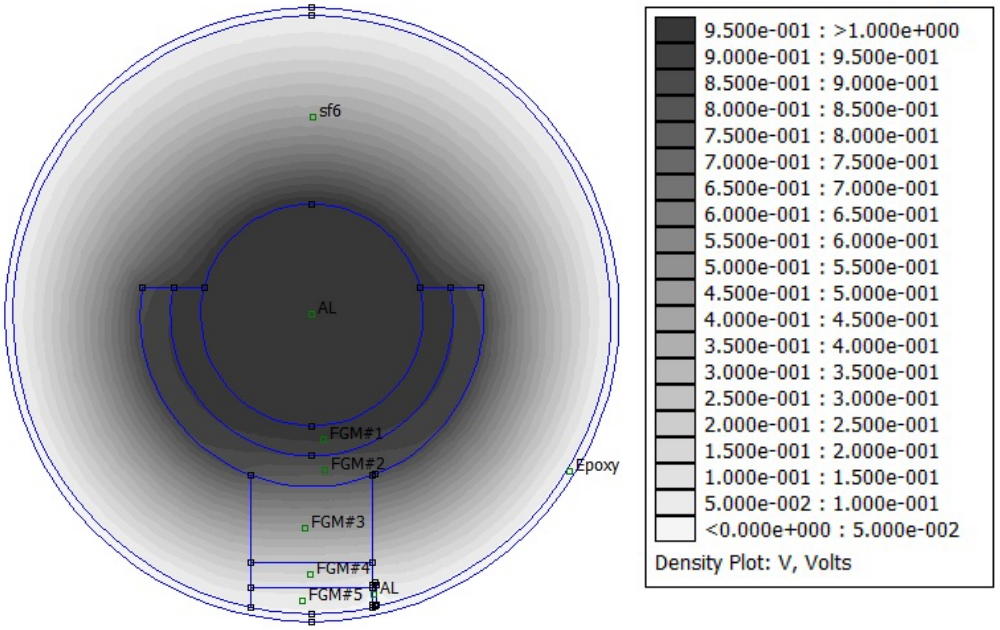

Figure 18. Electric Potential distribution along surface of FGM of disc spacer with single contaminating particle adhered to spacer inside gas insulated bus duct

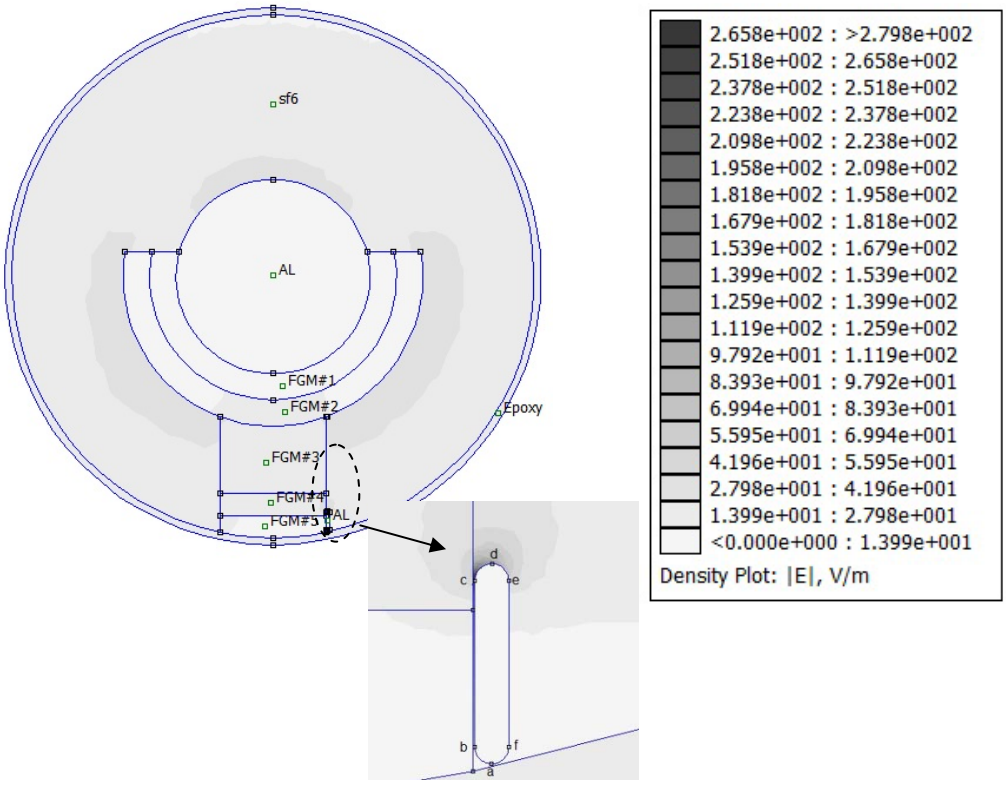

Figure 19. Electric field distribution along surface of FGM of disc spacer with single contaminating particle adhered to spacer inside gas insulated bus duct

Electric field distribution along particle length which adhered to uniform (Epoxy) or FGM of disc spacer is shown in Figure 20. It is seen that the electric field increases gradually from minimum value at

lower tip point (a) of particle until it reaches maximum value at triple junction point (c) but after that point, it decreases gradually through path (d-e-f) until it reaches the minimum value at lower tip point (a). From this figure, also it can be observed that the electric field is reduced at triple junction point(c) of particle with FGM spacer than it with uniform (Epoxy) spacer. Hence the field intensification at triple junction point (c) of particle is reduced by applying the U-shape FGM spacer.

Figure 21 shows Electric field distribution along upper gap space from triple junction point (c) of particle up to high voltage conductor. From this figure, it is found that the electric field decreases from maximum value at triple junction point (c) as far from particle until it reaches a certain value but after that point it slightly increased as it approached from high voltage conductor. The maximum electric field at triple junction point (c) of particle is reduced by about 10% with applying U-shape FGM spacer than it with uniform (Epoxy) spacer.

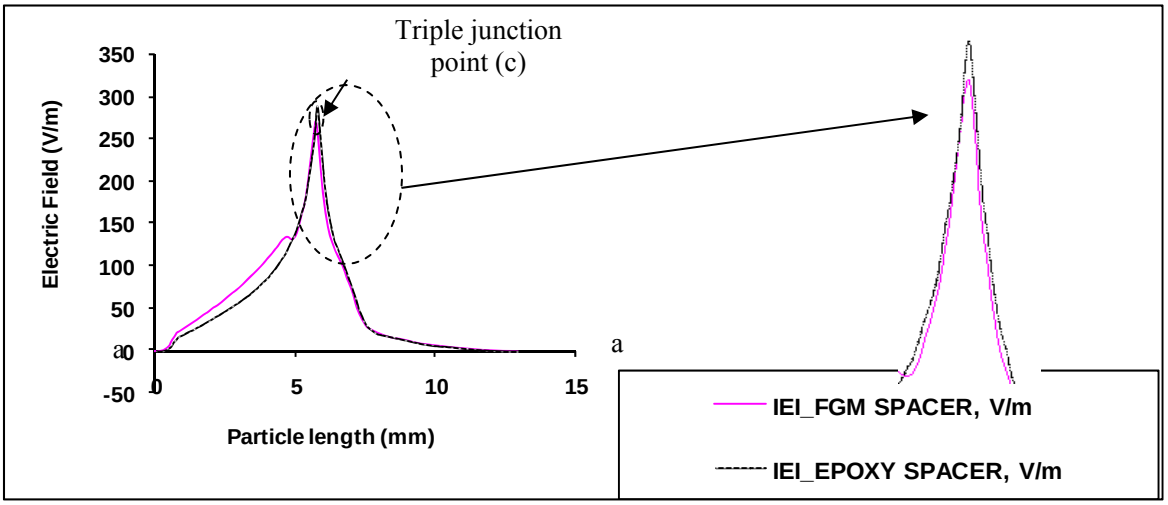

Figure 20. Electric field distribution along particle length which adhered to uniform (Epoxy) or FGM of disc spacer

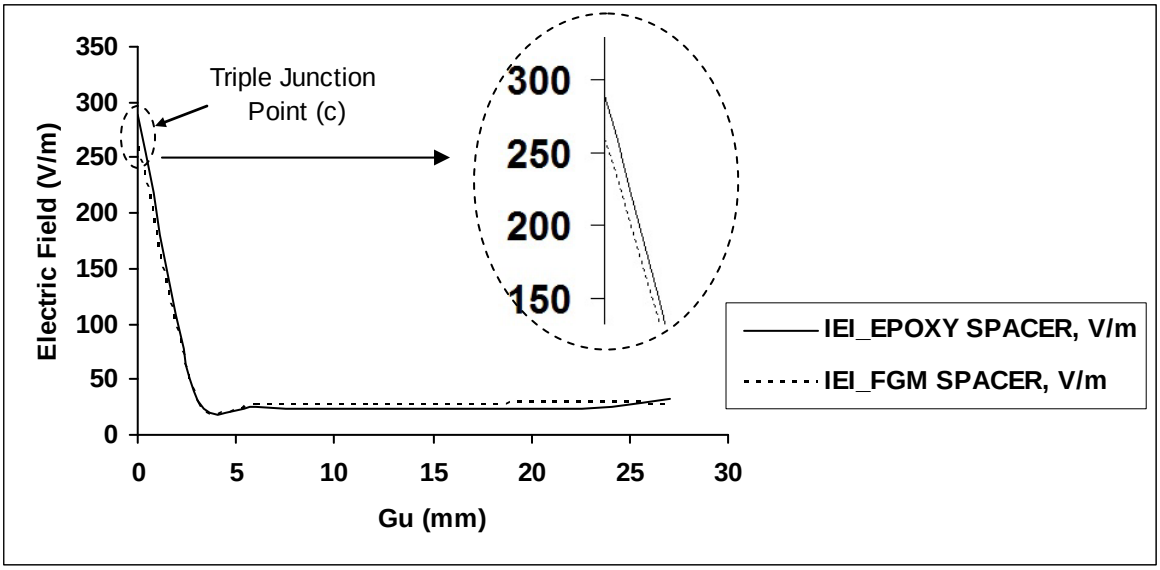

Figure 21. Electric field distribution along upper gap space from triple junction point (c) of particle up to high voltage conductor

(c) Electric field distribution along surface of FGM of disc spacer with multi-contaminating particles

The gas insulated bus duct with FGM of disc spacer and multi-contaminating particles is shown in Figure 22. The multi-contaminating particles are represented by two ground particles adhered to spacer and one protrusion rested at ground enclosure. All particles in this figure have the same length and radius as 5mm and 0.5 mm. Gu is defined as upper gap space from triple junction point of particle or upper tip up to high voltage conductor.

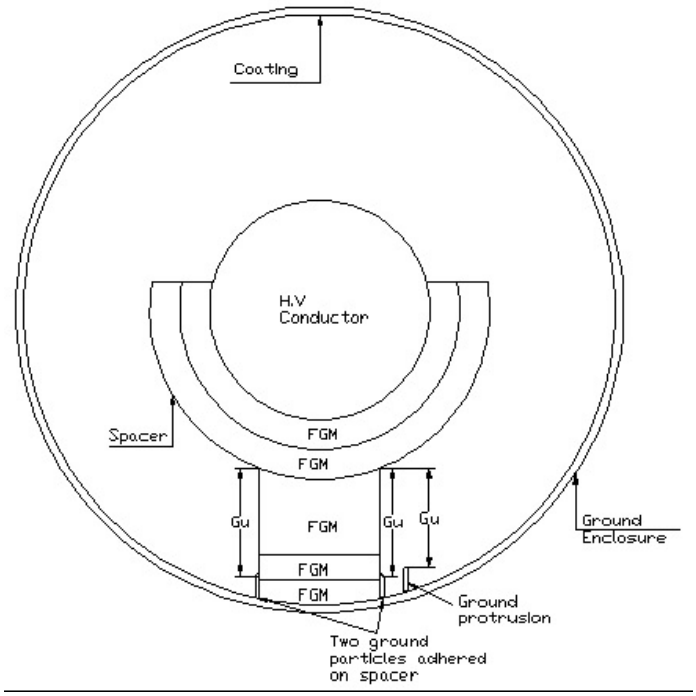

Figure 22. Gas insulated bus duct with FGM of disc spacer and multi- contaminating particles

Figure 23 shows the electric potential distribution along surface of FGM of disc- spacer with multi-contaminating particles inside gas insulated bus duct. It can be observed that the voltage increases gradually from 0V at ground enclosure through gap with disc spacer until it reaches 1V at high voltage conductor.

The electric field distribution along surface of FGM of disc-spacer with multi-contaminating particles inside gas insulated bus duct is shown in Figure 24. It is clear that, the electric field increases gradually from lower tip point (a) of particles until it reaches maximum value at triple junction point (c). From point (c) up to high voltage conductor, the electric field decreases gradually through gap as far from particle until it reaches a certain value and then it slightly increased as it approached from high voltage conductor.

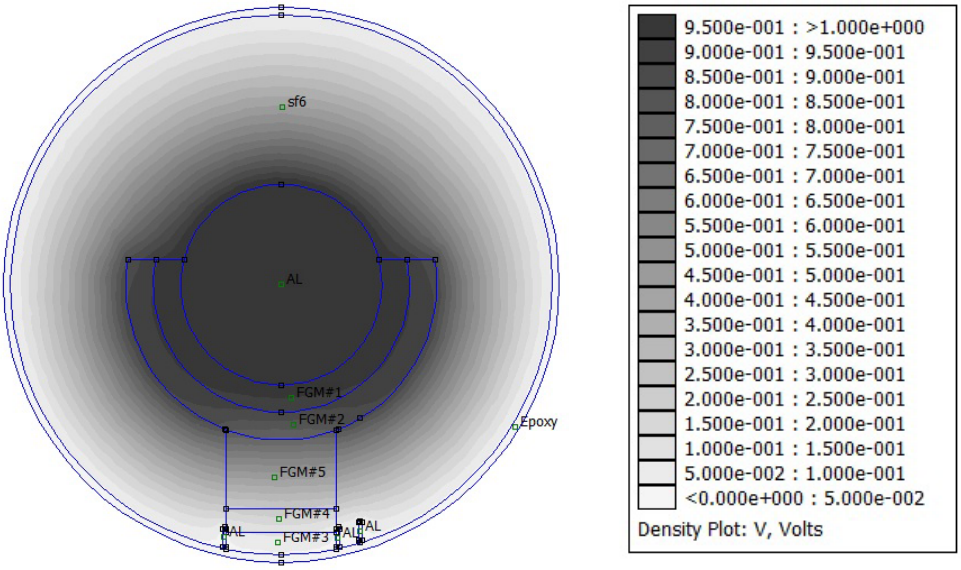

Figure 23. Electric Potential distribution along surface of FGM of disc spacer with multi-contaminating particles inside gas insulated bus duct

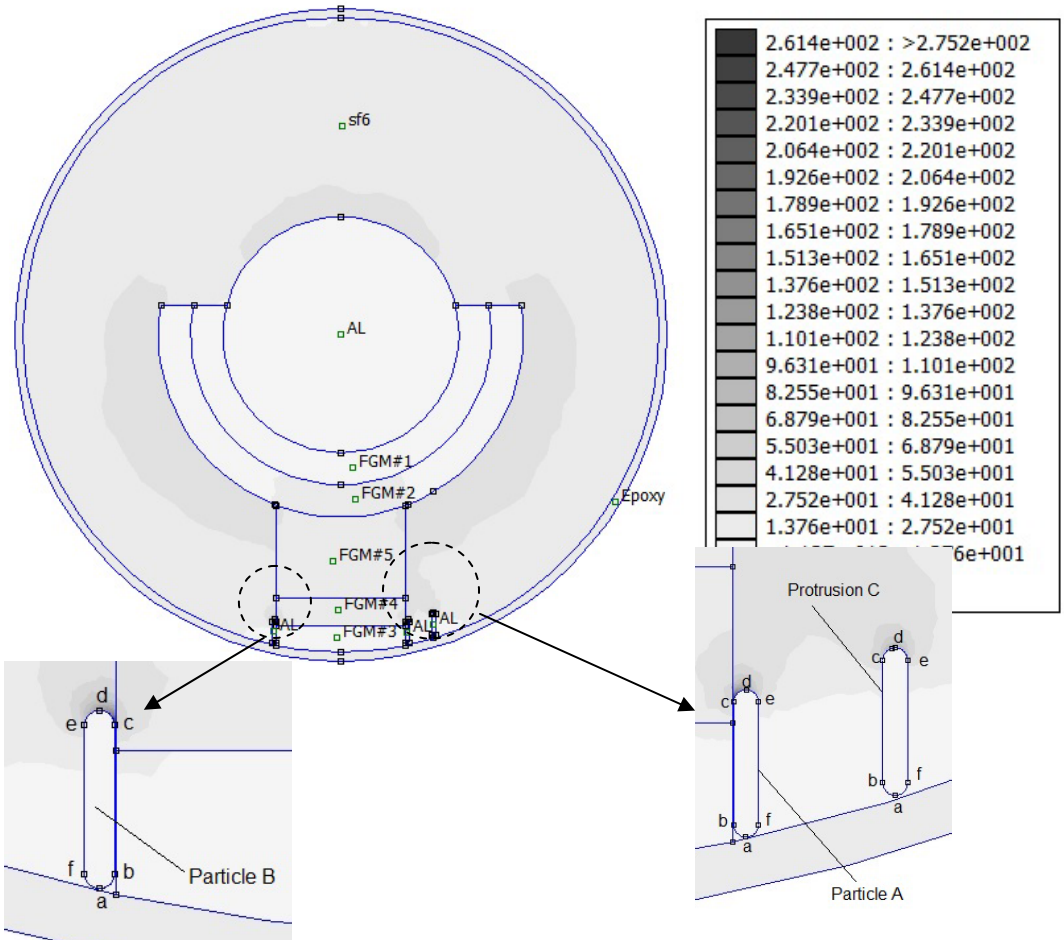

Figure 24. Electric field distribution along surface of FGM of disc spacer with multi-contaminating particles inside gas insulated bus duct.

Figure 25 shows Electric field distribution along length of two particles adhered to FGM spacer and other protrusion rested at ground enclosure. It is seen that the electric field increases gradually from minimum value at lower tip point (a) of particle until it reaches maximum value at triple junction point (c) of particles (A&B) and at upper tip point (d) of protrusion (C). After triple junction point (c) of particles (A&B) or upper tip point (d) of protrusion (C), the electric field decreases until it reaches minimum value at lower tip. Also it can be observed that the maximum electric field is observed at triple junction point of particle (B).

Electric field distribution along upper gap space from triple junction point (c) or upper tip point (d) of particles up to high voltage conductor is shown in Figure 26. It is clear that the electric field decreases from maximum value at triple junction point (c) of particles (A&B) or from upper tip of protrusion (C) as far from particles until it reaches a certain value but after that point it slightly increased as it approached from high voltage conductor. The maximum electric field is observed at triple junction point (c) of particle (B). The electric field at triple junction point (c) of particle (B) is greater than it at triple junction point (c) of particle (A) which is greater than it at upper tip point (d) of protrusion (C).

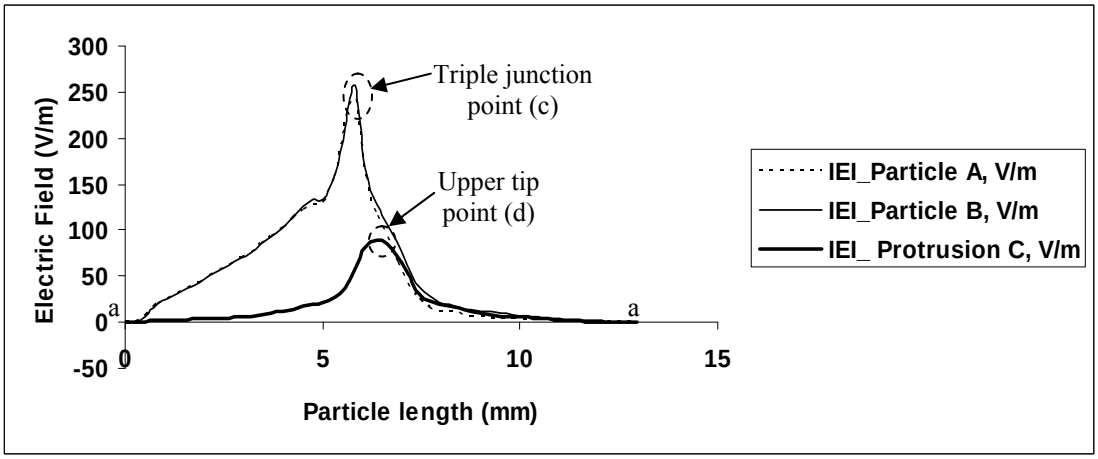

Figure 25. Electric field distribution along length of two particles adhered to FGM spacer and other protrusion rested at ground enclosure

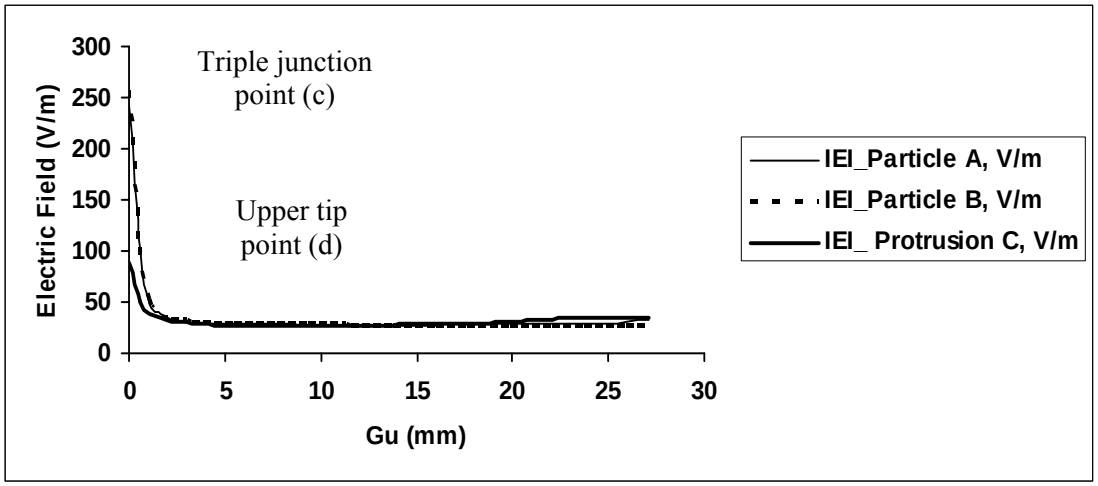

Figure 26. Electric field distribution along upper gap space from triple junction point (c) or upper tip point (d) of particle up to high voltage conductor

4. CONCLUSION

A new concept on solid spacers with keeping their simple structure and configuration, called a functionally graded material (FGM) is applied in this work to disc spacer to reduce the concentration of the maximum electric field at triple junction point of particle with spacer and gas which was one of the important factors dominating a long-term insulating property of the solid spacer. When it compared the effect of FGM spacer with uniform (Epoxy) spacer in case of gap without any particle contamination, it observed that the electric field at triple junction points which in contact with high voltage conductor and with ground enclosure in case of FGM spacer are reduced than that in case of Epoxy spacer. The electric field relaxation effects of 0.69 on high voltage electrode/spacer interface and 0.75 on ground electrode/spacer interface are achieved by applying the U-shape FGM spacer. The maximum electric field at triple junction point of particle which adhered to spacer is reduced by about 10% with applying U-shape FGM spacer than that of a uniform (Epoxy) spacer. In case of multi-contaminating particles with using FGM spacer, the electric field at triple junction point of particle which located at the left side of spacer is greater than that at triple junction point of particle which located at the right side of spacer in which is greater than that at upper tip point of protrusion. It is recommended to use FGM spacer instead of uniform (Epoxy) spacer for its great advantages to reduce field concentration at triple junction points which considered the dangerous point at gas insulated bus duct and can lead to breakdown of the insulated gas.

REFERENCES

[1] Rauno Gordon, Tuukka Arola, Katrina Wendel, Outi Ryynanen and Jari Hyttinen. "*Accuracy of numerical methods by calculating static and quasistatic electric fields*". Proc. Estonian Acad. Sci. Eng. 2006; 12: 262-283.

[2] Jawad Faiz, M Ojaghi. "'Instructive Review of Computation of Electric Fields using Different Numerical Techniques". *International Journal of Engineering*. 2002; 18(3): 344-356.

[3] E Kuffel, WS Zaengl and J Kuffel. "High Voltage Engineering Fundamentals". *Second edition*, *Butterworth-Heinemann Linacre House*, Jordan Hill, Oxford OX2 8DP, 225 Wildwood Avenue, Woburn, MA01801-2041. 2000: 246-254.

[4] David Meeker. "Finite Element Method Magnetics, Version 4.2, User's Manual". September 2006.

[5] CIGRE WG 15.03: "LONG-TERM PERFORMANCE OF SF6 INSULATED SYSTEMS", *CIGRE Report* 15-301, 2002.

[6] T Tanaka, T Okamoto, K Nakanishi and T Miyamoto. "Aging and Related Phenomena in Modern Electric Power Systems". *IEEE Trans.Dielectr. Electr. Insul*. 1993; 28(5): 826-844.

[7] MF Fréchette, CW Reed. "The Emerging Field of Nanodielectrics:an Annotated Appreciation". *IEEE Intern. Sympos. Electr. Insul. (ISEI)*. 2006: 458-465.

[8] T Tanaka, Y Ohki, M Ochi, M Harada and T Imai. "Enhanced Partial Discharge Resistance of Epoxy/Clay Nanocomposite Prepared by Newly Developed Organic Modification and Solubilization Methods". *IEEE Trans. Dielectr. Electr. Insul.* 2008; 15(1): 81-89.

[9] A Haddad and D Warne. "dvances in High Voltage Engineering". The Institution of Electrical Engineers UK, 2004.

[10] S Okabe, N Hayakawa, H Murase, H Hama, and H Okubo. "Common Insulating Properties in Insulating Materials". *IEEE Trans. Dielectr. Electr. Insul*. 2006; 13: 327-335.

[11] M Kurimoto, K Kato, H Adachi, S Sakuma, H Okubo. "Fabrication and experimental verification of permittivity graded solid spacer for GIS". *IEEE Conf. Electr. Insul. Dielectr. Phenomena (CEIDP)*. 2002: 789-792.

[12] H Okubo, M Kurimoto, H Shumiya, K Kato, H Adachi, S Sakuma. "Permittivity Gradient Characteristics of GIS Solid Spacer". *IEEE 7th Intern. Conf. Properties and Applications of Dielectric Materials(ICPADM)*. 2003: 23-26.

[13] H Shumiya, K Kato and H Okubo. "Feasibility Study on FGM (Functionally Graded Materials) Application for Gas Insulated Equipment". IEEE *Conf. Electr. Insul. Dielectr. Phenomena (CEIDP)*. 2004: 360-363.

[14] K Kato, M Kurimoto, H Shumiya, H Adachi, S Sakuma and H Okubo. "Application of Functionally Graded Material for Solid Insulator in Gaseous Insulation System". *IEEE Trans. Dielectr. Electr. Insul*. 2006; 13: 362-372.

[15] H Okubo, H Shumiya, M Ito and K Kato. "Optimization Techniques on Permittivity Distribution in Permittivity Graded Solid Insulators". *IEEE Intern. Sympos. Electr. Insul. (ISEI)*. 2006: 519-522.

[16] M Kurimoto, K Kato, M Hanai, Y Hoshina, M Takei, H Okubo. "Application of Functionally Graded Material for Reducing Electric Field on Electrode and Spacer Interface". *IEEE Trans. Dielectr. Electr. Insul.* 2010; 17(1): 256-263.

BIOGRAPHIES OF AUTHORS

Mousa A. Abd-Allah was born in Cairo, Egypt, on August 16, 1961. He received the B.Sc. degree in electrical Engineering with honor in 1984 and the M.Sc. degree in High Voltage Engineering in 1988, both from Zagazig university, benha branch, Cairo, Egypt. He received the Ph.D. degree in High Voltage Engineering in 1992 from Cairo university. He is currently a professor with the Electrical Engineering department, Faculty of Engineering at Shoubra, Benha university. His research activity includes Electromagnetic Field Assessment and Mitigation around Electrical Equipments, Gas discharge in gas insulated systems, Electromagnetic Compatibility, Transient Phenomenon in Power Networks.

Sayed A. Ward was born in Cairo, Egypt, on December 24, 1961. He received the B.Sc. degree in electrical engineering with honor in 1984 and the M.Sc. degree in high-voltage Engineering in 1988, both from Zagazig University, Shoubra, Cairo, Egypt. He received the Ph.D. degree in high-voltage engineering in 1992 from Cairo University. He is currently a professor with the Electrical Engineering Department, Faculty of Engineering (Shoubra), Cairo, Egypt. His research activity includes studying the gas discharge phenomena in GIS, breakdown voltage study in GIS systems for compressed gases and gas mixtures. Also his research activity includes breakdown in Insulating Oils and DGA oil analysis in power transformers.

Amr A. Youssef was born in Cairo, Egypt, on July 31, 1985. He received the B.Sc. degree in electrical engineering with honor degree in 2007 from Faculty of Engineering at Shoubra, Benha University, Cairo, Egypt. On December 2008, he received his work in this faculty as an instructor in the Electrical Engineering Department. In 2011, he will receive the M.Sc. degree in electrical engineering from this faculty. Currently he is an assistant lecturer at Electrical Engineering Department in this faculty and also PH.D researcher in high voltage engineering. His research activity includes studying the characteristics of various gas mixtures, electric field and breakdown voltage calculations around single and multi-contaminating particles inside GIS and GIBD.